plex manner. This may be due to the fact that the intrinsic intramolecular vibration frequencies of $Ni(NO_2)_6^{4-}$ are lower than those of $Co(NO_2)_6^{3-}$.

In the spectrum of $Na_2Ba[Ni(NO_2)_6]$ shown in Figure 2, the band around 200 cm^{-1} shifts considerably with a lowering of temperature. Such a frequency shift was also seen for the band at 214 cm^{-1} of $Na_3[Co(NO_2)_6]$. Therefore, the band around 200 cm^{-1} of $Na_2Ba[Ni(NO_2)_6]$ may be assigned to the lattice mode related to the Na^+ ion. The lowest band around 80 cm^{-1} which also exists in the spectrum of $K_2Ba[Ni(NO_2)_6]$ is assigned to the lattice mode related to the Ba^{2+} ion.

Conclusion

The far-infrared bands due to the lattice vibrations and the intramolecular vibrations of the hexanitro complex salts were both interpreted by the normal-coordinate analysis of the crystal as a whole, only the interaction between the outer cations and the oxygen atoms being taken into consideration. Low-temperature spectra yield useful information on the interpretation of the observed bands.

Lattice vibrations due to the displacements of the outer cations relative to the complex ion are observed below 200 cm^{-1}. Those frequencies change depending upon the mass of the cations and the interionic force constants. In order to establish the characteristic frequencies of the lattice vibrations arising from the outer cations, further investigations on the far-infrared spectra of various types of complex salts are in progress.

Appendix

For the intramolecular potential, V_{intra}, the modified Urey–Bradley force field (MUBFF) has been used and the use of this type of potential in the vibrational analysis of the complex ions has been fully discussed in several previous papers.[4b,12–14] Force constants used in the present study are summarized in Table VI, where K, H, and F denote the bond stretching, the angle deformation, and the repulsion between nonbonded atoms, respectively. F_{dia} means the diagonal element of the **F** matrix (potential energy matrix) for the corresponding mode. $p(NO,NO)$ is the resonance interaction constant. The value of $p(MN,MN)$ cannot be determined unless the frequencies of the g species are available.

TABLE VI

INTRAMOLECULAR POTENTIAL CONSTANTS (MDYN/Å) FOR $Co(NO_2)_6^{3-}$ AND $Ni(NO_2)_6^{4-}$ [a]

	$Co(NO_2)_6^{3-}$	$Ni(NO_2)_6^{4-}$
F_{dia}(MN str)	1.50	0.80
F_{dia}(NO str)	9.30	9.30
F_{dia}(NMN def)	1.10	0.60
F_{dia}(ONO def)	1.78	2.00
F_{dia}(MNO def)	0.50	0.40
	0.30 (Na salt)	
F_{dia}(NO_2 wag)	0.55	0.32
F_{dia}(NO_2 twist)	0.03 (assumed)	0.03
$F(N\cdots N)$	0.05	0.20[b]
$F(O\cdots O)$	3.00	3.00
$F(M\cdots O)$	0.20	0.10
p(NO,NO)	0.50	0.50

[a] In the Urey–Bradley approach, diagonal elements of the **F** matrix corresponding to the bond stretching modes include F as well as K and those for angle deformation modes include F as well as H. The off-diagonal elements are expressed in terms of F.
[b] Taking into account the appreciable interaction between the Ni–N stretching and NMN deformation modes, the effective value of $F(N\cdots N)$ was assumed to be large.[4b,12]

CONTRIBUTION FROM BELL TELEPHONE LABORATORIES, INC.
MURRAY HILL, NEW JERSEY 07971

Rare Earth Orthogallates

BY M. MAREZIO, J. P. REMEIKA, AND P. D. DERNIER

Received November 9, 1967

Single crystals of the rare earth orthogallates, $REGaO_3$ with RE = Sm–Lu, have been synthesized by the decomposition of the respective garnets at high pressure in the presence of a flux. Previously reported crystals of $LaGaO_3$, $PrGaO_3$, and $NdGaO_3$ have been prepared by the flux method at atmospheric pressure. The rare earth orthogallates are isostructural with the rare earth orthoferrites; namely, they have the orthorhombic perovskite-like structure. Their lattice parameters have been calculated by the least-squares method. The parameters a and c increase smoothly in going from Lu to La. However, the lattice parameter b goes through a maximum. It seems that this anomalous variation of the b parameter can be explained in terms of a variation of the coordination number of the rare earth cation.

Introduction

In a recent note[1] we reported the synthesis and the crystal structure of $GdGaO_3$, $YbGaO_3$, and $YGaO_3$. They were synthesized by decomposition at high pressure and high temperature of the respective garnets. The new orthogallates are isostructural with the respective orthoferrites; namely, they have the orthorhombic perovskite-like structure. An interesting feature is that the rare earth orthoferrites can be synthesized at atmospheric pressure, whereas a pressure greater than 45 kbars is needed to synthesize $GdGaO_3$, $YbGaO_3$, and $YGaO_3$. This was explained in terms of

---

(1) M. Marezio, J. P. Remeika, and P. D. Dernier, *Mater. Res. Bull.*, **1**, 247 (1966).

the stronger preference of the Ga^{3+} ions for the tetrahedral sites in oxide compounds. If a mixture of RE$_2$O$_3$ (RE = Sm–Lu) and Ga$_2$O$_3$ is fired at atmospheric pressure, the corresponding garnet RE$_3$Ga$_5$O$_{12}$ is obtained. In the garnet structure three-fifths of the galliums are tetrahedrally coordinated and two-fifths octahedrally coordinated. All of the gallium ions in the REGaO$_3$ compounds are in octahedral sites.

The present paper, which is part of a continuing program of study of the Ga^{3+} crystal chemistry in our laboratory, reports the synthesis and the crystal data of all the rare earth orthogallates.

Experimental Section

With the exception of LaGaO$_3$, PrGaO$_3$, and NdGaO$_3$, single crystals of all the other rare earth orthogallates were prepared by subjecting the respective garnets to high pressure and high temperature in the presence of a NaOH flux. The high-pressure runs were made by following the same procedure that has been described in detail earlier.[1] This time the temperature was monitored with a Pt—Pt–10% Rh thermocouple during each experiment. At high pressure the temperature fluctuation was less than ±20° at 1000°. No correction was made for the effect of pressure on the thermocouple. A temperature of 1000° and a pressure of 45 kbars proved to be sufficient for the decomposition of all the rare earth gallium garnets. It is interesting to note that under the above conditions complete decomposition was obtained from Sm$_3$Ga$_5$O$_{12}$ to Tb$_3$Ga$_5$O$_{12}$, whereas a partial decomposition was obtained from Dy$_3$Ga$_5$O$_{12}$ to Lu$_3$Ga$_5$O$_{12}$, as evidenced by the occurrence of lines belonging to the garnet structure in the X-ray photographs of the quenched materials.

The first three members of the orthogallate series, namely, LaGaO$_3$, PrGaO$_3$, and NdGaO$_3$, can be synthesized at normal pressure. Their synthesis and crystal data have been reported previously.[2] Since it was our interest to have a complete set of lattice parameters of the orthogallates, we have prepared these materials and redetermined their lattice parameters. Single crystals were grown by self-nucleation from a melt starting at 1300° and consisting of the stochiometric proportions of the constituent oxides, which were of 99.99% purity by emission spectroscopic analysis. The PbO(B$_2$O$_3$)$_x$ flux used was of the same purity level. Cooling rates were of the order of 1–5°/hr. Complete details of the crystal growth of the ABO$_3$ perovskite-like compounds from the flux system PbO(B$_2$O$_3$)$_x$ will be published elsewhere.

Three compounds were selected for compositional analysis. Atomic absorption analysis gave 51.8% La and 26.0% Ga for LaGaO$_3$ and 54.9% Nd and 25.0% Ga for NdGaO$_3$, compared with the calculated values 54.13% La, 27.17% Ga and 55.07% Nd, 26.61% Ga. X-Ray fluorescence analysis for SmGaO$_3$ gave 56.7% Sm and 24.5% Ga compared with the calculated values 56.09% Sm and 26.01% Ga. In the case of the crystals grown from the NaOH flux at high pressure, an emission spectroscopic analysis was performed for Na and it indicated that Na is present as a negligible impurity in the range of $0.000X\%$.

The X-ray powder photographs were taken at room temperature ($\sim$24°) with a Norelco camera of 114.6-mm diameter and Zr-filtered Cr radiation (Kα_1 2.28962 Å and Kα_2 2.29352 Å) The photographs were indexed on the basis of the orthorhombic cell with the lattice constants given in Table I. There was some doubt about the pattern of LaGaO$_3$. It could have been indexed on the trigonal cell isostructural with the one of LaAlO$_3$. After taking long exposure photographs with Cr Kα and one with Cu Kα, lines that could have only been explained with the orthorhombic cell appeared in the photographs. The final lattice parameters were obtained by accurate measurements of the 2θ values for at least ten reflections in the back reflection region. Those reflections for which overlapping could occur were discarded. The least-squares refinement program of Mueller, *et al.*,[3] was used. The powder diffraction data for all of the compounds are listed in Table II, where the reflections that were unobserved throughout the whole series have been omitted.

Table I

Crystallographic Data of the REGaO$_3$[a]

	Orthorhombic cell				Pseudo-cell		
	a, Å	b, Å	c, Å	Vol Å^3	$a = c$, Å	b, Å	β, deg
LaGaO$_3$	5.526	5.473	7.767	234.9	3.888	3.884	90.6
PrGaO$_3$	5.458	5.490	7.733	231.7	3.871	3.866	90.3
NdGaO$_3$	5.431	5.499	7.710	230.3	3.865	3.855	90.7
SmGaO$_3$	5.369	5.520	7.650	226.7	3.850	3.825	91.6
EuGaO$_3$	5.351	5.528	7.628	225.6	3.847	3.814	91.9
GdGaO$_3$	5.322	5.537	7.606	224.1	3.840	3.803	92.3
TbGaO$_3$	5.307	5.531	7.578	222.4	3.833	3.789	92.4
DyGaO$_3$	5.282	5.534	7.556	220.9	3.825	3.778	92.7
HoGaO$_3$	5.251	5.531	7.536	218.9	3.813	3.768	93.0
ErGaO$_3$	5.239	5.527	7.522	217.8	3.808	3.761	93.1
TmGaO$_3$	5.224	5.515	7.505	216.2	3.798	3.753	93.1
YbGaO$_3$	5.208	5.510	7.490	214.9	3.791	3.745	93.2
LuGaO$_3$	5.188	5.505	7.484	213.7	3.782	3.742	93.4

[a] The observed standard deviation of the lattice parameters determined in the present work was in all cases less than 1/12,000. As a conservative estimate of limits of error we consider the values of all parameters to be accurate within a precision of 1/5000.

Details of the structural arrangement of the orthorhombic distortion of the perovskite structure are given by Coppens and Eibschütz,[4] who refined the structure of YFeO$_3$.

Discussion

In Figure 1 the lattice parameters of the rare earth orthogallates are plotted against the atomic number of the rare earth. Within experimental error the a and c parameters increase smoothly in going from Lu to La. Instead, the b parameter has an unexpected behavior. It goes through a maximum at about Dy–Tb–Gd. As shown by Eibschütz,[5] the lattice parameters of the corresponding rare earth orthoferrites have the same behavior. In this case the b parameter goes through a maximum at Gd. No explanation was given to account for this anomalous variation.

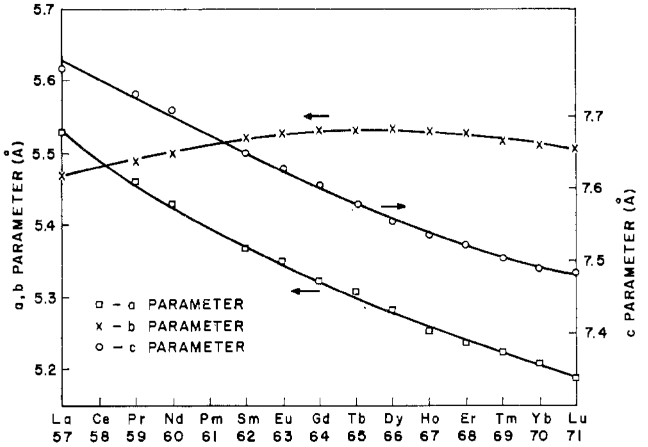

Figure 1.—Lattice parameters a, b, and c *vs.* atomic number for the rare earth orthogallates.

In the "ideal perovskite" ABO$_3$ compounds the A^{3+}

---

(2) S. Geller, *Acta Cryst.*, **10**, 243 (1957).

(3) M. H. Mueller, L. Heaton, and R. T. Miller, *ibid.*, **13**, 828 (1960).

(4) P. Coppens and M. Eibschütz, *ibid.*, **19**, 524 (1965).

(5) M. Eibschütz, *ibid.*, **19**, 337 (1965).

Table II

Powder Diffraction Data for Some Rare Earth Orthogallates

hkl	La			Pr			Nd			Sm			Eu		
	d_o(A)	d_c	I_o	d_o	d_c	I_o	d_o	d_c	I_o	d_o	d_c	I_o	d_o	d_c	I_o
110	3.865	3.888	vvw	3.842	3.871	vw	3.840	3.864	w	3.828	3.849	w	3.818	3.845	w
002															
111	3.463	3.477	vvw	3.442	3.461	vw	3.441	3.454	w	3.426	3.438	w	3.421	3.433	wm
020							2.744	2.749	w	2.749	2.760	m	2.755	2.764	m
112	2.722	2.748	vs	2.723	2.736	s	2.720	2.729	s	2.707	2.713	s	2.701	2.708	s
200										2.678	2.685	m	2.668	2.676	m
021				2.576	2.587	vw	2.583	2.590	w	2.590	2.596	w	2.592	2.599	wm
211					2.333			2.321			2.302		2.292	2.297	w
103	2.339	2.344	w	2.322	2.330	w	2.318	2.323	w	2.300	2.303	w		2.297	
022	2.237	2.237	wm	2.227	2.238	wm	2.233	2.238	wm	2.233	2.238	w	2.233	2.238	w
202							2.216	2.220	wm	2.197	2.197	w	2.187	2.190	w
113				2.137	2.146	w	2.137	2.140	w	2.123	2.126	w	2.116	2.121	w
122	2.073	2.074	vvw												
220	1.940	1.944	s	1.929	1.935	m	1.927	1.932	ms	1.922	1.924	m	1.919	1.923	m
004		1.942			1.933			1.928		1.910	1.913	m	1.904	1.907	m
023															
221	1.883	1.886	vw	1.873	1.877	w	1.871	1.874	wm	1.865	1.866	m	1.863	1.864	wm
213	1.783	1.786	vw												
301															
114				1.725	1.729	vw	1.721	1.725	vw						
131	1.692	1.691	vw	1.689	1.693	w	1.692	1.694	wm	1.694	1.697	m	1.696	1.699	m
310														1.698	
311							1.677	1.678	vw	1.661	1.662	vw	1.657	1.657	w
132	1.584	1.582	s	1.580	1.583	m	1.579	1.583	m	1.582	1.584	m	1.582	1.585	m
024		1.584			1.581			1.578		1.570	1.572	m	1.568	1.570	m
204	1.590	1.589	s	1.575	1.578	m	1.568	1.572	ms	1.556	1.558	s			
312		1.592			1.577			1.570			1.555		1.550	1.551	s
223				1.545	1.548	vw	1.542	1.544	vw	1.535	1.536	w	1.532	1.533	w
231	1.494	1.494	vw												
105		1.495													
303															
133				1.438	1.439	w	1.437	1.439	wm	1.437	1.438	m	1.436	1.437	m
115	1.441	1.443	vw												
232															
313															
040				1.372	1.373	vw	1.373	1.375	w	1.378	1.380	w	1.381	1.382	w
322															
041				1.350	1.351	vw							1.359	1.360	w
224	1.374	1.374	ms	1.366	1.368	m	1.363	1.364	m	1.356	1.357	s	1.353	1.354	m
140															
025															
400	1.380	1.381	m				1.357	1.358	w	1.343	1.342	w	1.337	1.338	w
233															
042															
134															
215															
330															
411															
006															
142															
331				1.272	1.273	w	1.270	1.270	wm	1.265	1.265	wm	1.264	1.264	m
240				1.226	1.226	wm	1.226	1.226	w	1.227	1.227	w	1.228	1.228	w
043				1.211	1.212	wm	1.211	1.212	wm				1.214	1.214	m
241					1.211			1.211					1.212	1.212	w
332	1.231	1.230	m	1.224	1.224	m	1.221	1.222	m	1.217	1.216	m	1.214	1.215	m
116	1.229	1.228	ms	1.222	1.223	ms	1.219	1.219	ms	1.211	1.210	s	1.207	1.207	ms
420	1.233	1.233	m		1.222		1.217	1.217	w				1.205	1.204	w
225	1.214	1.214	vw				1.205	1.205	w	1.198	1.198	w	1.195	1.195	m
143															
421							1.202	1.202	vw	1.193	1.192	w	1.189	1.189	m
324															
242													1.169	1.169	vw
026										1.158	1.158	vw			
305							1.173	1.174	vw	1.163	1.163	vw			
413	1.190	1.190	vw					1.173					1.158	1.158	w
206	1.172	1.172	w	1.165	1.165	w				1.152	1.152	vw		1.148	
422	1.176	1.175	w		1.165						1.151		1.148	1.148	ms
135				1.155	1.155	wm	1.153	1.153	m	1.149	1.149	m		1.148	
315	1.161	1.161	w												
333	1.159	1.159	w	1.154	1.154	wm	1.151	1.151	m						

hkl	Tb			Dy			Ho			Er			Tm			Lu		
	d_o	d_c	I_o	d_o	d_c	I_o	d_o	d_c	I_o	d_o	d_c	I_o	d_o	d_c	I_o	d_o	d_c	I_o
110	3.809	3.829	w	3.811	3.821	w	3.790	3.808	w	3.788	3.802	w	3.780	3.793	w	3.747	3.775	w
002	3.772	3.789	w	3.766	3.778	w	3.747	3.768	w	3.745	3.761	w	3.733	3.753	w	3.709	3.742	w
111	3.403	3.418	m	3.398	3.410	m	3.382	3.399	m	3.375	3.393	m	3.369	3.385	m	3.343	3.371	m
020	2.775	2.765	m	2.757	2.767	m	2.737	2.765	s	2.731	2.763	ms	2.726	2.757	s	2.736	2.752	m
112	2.686	2.693	s	2.680	2.686	s	2.671	2.678	s	2.669	2.674	s	2.659	2.668	s	2.640	2.658	s
200	2.645	2.654	m	2.635	2.641	m	2.620	2.625	w	2.616	2.620	wm	2.606	2.612	wm	2.576	2.594	m
021	2.591	2.596	w	2.594	2.598	m	2.586	2.596	w	2.585	2.594	wm	2.579	2.588	wm			
211	2.275	2.281	w	2.271	2.273	w	2.257	2.266	w	2.254	2.262	w	2.245	2.252	vw	2.232	2.239	w
103		2.280			2.273			2.262			2.258			2.256				
022	2.229	2.234	w	2.227	2.232	vw				2.227	2.227	w						
202	2.168	2.174	m	2.163	2.164	w	2.150	2.154	w	2.145	2.150	w	2.138	2.144	w	2.124	2.132	wm
113	2.105	2.109	m	2.102	2.103	m	2.094	2.097	wm	2.089	2.093	w	2.085	2.088	w	2.074	2.081	wm
122																2.033	2.039	vw
220	1.912	1.915	m	1.908	1.910	m	1.902	1.904	m	1.899	1.901	m	1.894	1.896	wm	1.882	1.887	m
004	1.891	1.895	m	1.887	1.889	m	1.882	1.884	m	1.879	1.881	m	1.875	1.876	w	1.865	1.871	m
023	1.863	1.865	w	1.861	1.862	wm	1.856	1.859	m	1.856	1.857	m	1.851	1.853	w	1.844	1.848	m
221	1.852	1.856	m	1.850	1.852	m	1.844	1.846	m	1.842	1.843	m	1.836	1.839	wm	1.826	1.830	m
213	1.734	1.737	vw															
301							1.701	1.705	ms	1.700	1.701	m	1.697	1.696	ms			
114																1.673	1.676	vw
131	1.696	1.697	m	1.695	1.697	m	1.692	1.695	m	1.693	1.693	m	1.688	1.690	w	1.682	1.685	m
310				1.679	1.678	vw	1.668	1.669	w	1.665	1.665	w	1.664	1.661	vw	1.645	1.649	vw
311	1.644	1.645	vw	1.636	1.638	w	1.630	1.629	vw	1.623	1.626	w	1.620	1.621	vw	1.609	1.611	w
132	1.580	1.582	m	1.579	1.581	m	1.578	1.579	m	1.576	1.578	m	1.572	1.574	wm	1.567	1.570	m
024	1.561	1.563	m	1.559	1.560	m	1.556	1.557	m	1.553	1.555	m	1.550	1.551	wm	1.544	1.547	m
204							1.533	1.531	m	1.527	1.528	wm	1.523	1.524	m	1.514	1.517	m
312	1.538	1.540	ms	1.533	1.533	ms	1.526	1.526	m	1.521	1.523	ms	1.516	1.519	m	1.506	1.509	ms
223	1.525	1.526	w	1.522	1.522	wm	1.517	1.517	w	1.513	1.515	w	1.509	1.511	vw			
231																		
105																		
303																1.420	1.421	m
133	1.432	1.434	m	1.431	1.432	m	1.430	1.430	m	1.427	1.428	m	1.424	1.425	m		1.422	
115				1.404	1.405	vw	1.401	1.401	vw	1.398	1.399	vw				1.389	1.391	w
232					1.404			1.401			1.399						1.391	
313				1.396	1.396	vw	1.391	1.390	vw							1.375	1.376	w
040				1.382	1.383	vw											1.376	
322					1.382													
041	1.360	1.360	m	1.360	1.361	m	1.360	1.360	wm	1.358	1.359	m	1.355	1.356	w	1.352	1.353	m
224	1.347	1.347	ms	1.342	1.343	m	1.339	1.339	s	1.336	1.337	s	1.335	1.334	s	1.327	1.329	ms
140											1.336			1.333				
025				1.326	1.326	vw	1.324	1.323	w	1.321	1.321	w	1.319	1.318	w	1.314	1.315	w
400	1.327	1.327	m	1.320	1.320	w	1.314	1.313	w	1.309	1.310	m	1.305	1.306	m	1.296	1.297	w
233	1.300	1.299	vw	1.298	1.296	vw												
042		1.299			1.299											1.291	1.292	w
134	1.281	1.282	vw															
215		1.280																
330							1.266	1.269	vw	1.267	1.267	vw	1.262	1.264	w			
411	1.272	1.272	vw										1.253	1.253	w			
006																1.247	1.247	w
142							1.261	1.260	vw									
331	1.259	1.259	m	1.255	1.256	m	1.252	1.252	m	1.249	1.250	m	1.247	1.247	m	1.241	1.241	m
240	1.227	1.226	w	1.225	1.225	vw												
043	1.213	1.213	w	1.212	1.213	w	1.211	1.211	m	1.210	1.210	w	1.207	1.207	w	1.205	1.205	m
241	1.211	1.210	m	1.209	1.210	w	1.208	1.208	m	1.206	1.206	m	1.204	1.203	m	1.200	1.200	ms
332				1.207	1.207	w	1.203	1.203	m	1.201	1.201	m	1.198	1.198	m	1.192	1.193	m
116	1.200	1.199	s	1.196	1.196	ms	1.193	1.193	ms	1.190	1.191	ms	1.188	1.188	ms	1.184	1.184	s
420	1.197	1.196	m	1.191	1.192	m	1.187	1.196	m	1.183	1.184	m	1.180	1.180	m		1.173	
225	1.189	1.188	m	1.185	1.185	m	1.182	1.182	m	1.179	1.180	m	1.177	1.177	m	1.173	1.173	s
143	1.182	1.182	m								1.179			1.177			1.174	
421		1.182		1.177	1.177	m	1.171	1.171	m	1.169	1.169	m	1.166	1.166	m	1.159	1.159	m
324	1.172	1.171	vw	1.167	1.168	w										1.153	1.153	w
242				1.166	1.166	w	1.164	1.164	m	1.163	1.162	m	1.160	1.160	m	1.156	1.156	m
026																		
305																		
413																		
206																		
422																		
135																		
315																		
333																		

ions are surrounded by 12 equidistant oxygen ions. In the orthorhombic distortion these 12 distances vary over a very large range; in fact, it is difficult to decide the coordination number of the cation A^{3+}. Of all the orthorhombic perovskite-like compounds, only two have been refined, $GdFeO_3$[4,6] and $YFeO_3$.[4] Although yttrium is not a rare earth, $YFeO_3$ can be considered an orthoferrite whose A cation falls between Dy and Ho in size. From the rare earth–oxygen distances in these compounds it can be seen that there are eight first nearest oxygens and four second nearest oxygens. The averages of the distances of the first nearest oxygens in $GdFeO_3$ and $YFeO_3$ are 2.48 and 2.43 Å, respectively. The averages of the distances of the other four oxygens are 3.39 and 3.45 Å, while the averages of the distances of all 12 oxygens are 2.78 and 2.77 Å, respectively. The four second nearest oxygens are closer to Gd in $GdFeO_3$ than to Y in $YFeO_3$. Therefore, the anomalous behavior of the *b* parameter in the $AFeO_3$ perovskite-like compounds, as A varies from Lu to La, can be explained if one considers the effect of the variation of the size of the A cation on the first nearest oxygens together with the effect of the same variation on the second nearest oxygens. As the size of A^{3+} increases, the average A–O distance of the first nearest oxygens increases, whereas the average A–O distance of the second nearest oxygens decreases. Therefore the unit cell increases and decreases, respectively. Since the *a* and *c* parameters vary smoothly across the series, only the *b* parameter is appreciably affected by this double effect. The *b* parameter increases on going from Lu to Gd because in this region the first effect is the predominant one, whereas it decreases on going from Gd to La because in this region the second effect is the predominant one.

The fact that the average A–O distance of the second nearest oxygens becomes smaller on going from $LuFeO_3$ to $LaFeO_3$ seems to suggest that the coordination number of the cation A^{3+} varies across the series. Even though $LaFeO_3$ is the least distorted among the rare earth orthoferrites, it can be seen from the intensities of the reflections in the powder pattern that the distortion from the ideal perovskite is still very appreciable which means that the coordination number should be far from 12.

It is reasonable to assume that the same explanation holds true in the case of the orthogallates.

The same behavior of the *b* parameter is also present in the rare earth orthochromites,[2,7] orthovanadites,[2,8] and orthorhodites.[9] In the case of orthoalumi-

---

(6) S. Geller, *J. Chem. Phys.*, **24**, 1236 (1956).

(7) S. Quezel-Ambrunaz and M. Mareshal, *Bull. Soc. Franc. Mineral. Crist.*, **86**, 204 (1963).

(8) B. Reuter, *Bull. Soc. Chim. France*, 1053 (1965).

(9) R. Chazalon, E. F. Bertaut, and T. Q. Duc, *Bull. Soc. Franc. Mineral. Crist.*, **87**, 98 (1964).

nates[10,11] the *b* parameter decreases slightly on going from $TmAlO_3$ to $SmAlO_3$. Starting with $NdAlO_3$, the orthoaluminates have the hexagonal perovskite-like arrangement.[10] In the cases of orthoscandates[2,11] and orthoindates[12] the *b* parameter increases throughout the series from Lu to La. These results seem to indicate that when the B cation of the ABO_3 perovskite-like compounds is a larger ion such as indium or scandium, the substitution of the A cation with a larger rare earth does not have an appreciable effect on the second nearest oxygens. Therefore, the coordination number of the rare earth probably varies across the series $REBO_3$ when B = Al, Ga, Fe, Cr, or V, whereas it is almost constant when B = Sc or In.

We plan to do the refinements of a number of these perovskite-like structures.

Acknowledgments.—We wish to thank T. Kometani and Miss S. Vincent for chemical analysis and E. M. Kelly for technical assistance in the crystal growth.

---

(10) S. Geller and V. B. Bala, *Acta Cryst.*, **9**, 1019 (1956).

(11) S. J. Schneider, R. S. Roth, and J. L. Waring, *J. Res. Natl. Bur. Std.*, **A65**, 345 (1961).

(12) R. D. Shannon, *Inorg. Chem.*, **6**, 1474 (1967).

CONTRIBUTION FROM THE DEPARTMENT OF CHEMISTRY,
MICHIGAN STATE UNIVERSITY, EAST LANSING, MICHIGAN 48823

The Crystal Structure of Lanthanum Carbonate Octahydrate

BY DENNIS B. SHINN AND HARRY A. EICK

Received November 6, 1967

The crystal structure of lanthanum carbonate octahydrate, $La_2(CO_3)_3 \cdot 8H_2O$, has been determined from an X-ray diffraction study of a single-crystal specimen. Four formula units are contained in the orthorhombic unit cell, space group Pccn, with lattice parameters $a = 8.984 \pm 0.004$, $b = 9.580 \pm 0.004$, and $c = 17.00 \pm 0.01$ Å ($\rho_{obsd} = 2.72 \pm 0.02$ g cm^{-3}; $\rho_{calcd} = 2.732$ g cm^{-3}). The final *R* factor was 0.061 for three-dimensional counter data collected with Cu Kα radiation [$(\sin \theta)/\lambda \leq 0.50$]. $La_2(CO_3)_3 \cdot 8H_2O$ crystallizes in an irregular layer type of structure in which the basic layer is formed by alternate rows of carbonate ions and metals. The structure contains two distinctive 10-coordinate metal polyhedra in which coordination sites are occupied both by water molecules and by bidentate and unidentate carbonates. The polyhedra symmetry may be related to a dodecahedron with two sites occupied by bidentate carbonate ions. One-fourth of the water molecules are not bound to the metal ions and are situated between the layers. The average La–O bond is 2.61 Å; individual La–O distances range from 2.52 to 2.74 Å. Hydrogen bonding is apparent.

Introduction

Methods of preparation, thermal decomposition, and structural properties of lanthanon carbonates have been the subject of numerous recent studies.[1-10] Unfortunately, many of these results and their interpretation are contradictory. The inconsistencies are due in part to preparatory difficulties and lack of structural data. A popular method for the preparation of the carbonates is homogeneous precipitation by hydrolysis of the trichloroacetate (eq 1) described first by Salutsky and Quill.[1]

$$2M(C_2Cl_3O_2)_3 + (x + 3)H_2O \longrightarrow M_2(CO_3)_3 \cdot xH_2O + 3CO_2 + 6HCCl_3 \quad (1)$$

By use of this and related methods, normal carbonates, $M_2(CO_3)_3 \cdot xH_2O$, have been prepared for all the lanthanons.[2-7] Values reported for *x* vary from 8 for the lighter metals to 2 or 3 for the heavier ones and also seem dependent on the preparatory conditions. In thermal decomposition studies of the hydrates, intermediate phases have not been observed consistently.[2-4,6,8] The crystal structures of the lanthanon carbonates are unknown, although many reported lattice parameters are based on values analogous to those obtained from a single crystal of lanthanite[11] $\{(La, Ce)_2(CO_3)_3 \cdot 8H_2O\}$.

In order to determine the structural interrelationships in the lanthanon carbonates and to resolve some of the contradictory reports of their properties, a single-crystal X-ray diffraction study of the inherent structures has been initiated. The structure of $La_2(CO_3)_3 \cdot 8H_2O$ is described below.

Experimental Section

Crystals of lanthanum carbonate octahydrate, $La_2(CO_3)_3 \cdot 8H_2O$, prepared by slow hydrolysis of lanthanum trichloroacetate, were obtained from Dr. L. L. Quill of this department. Composition was determined from carbon and hydrogen analyses (Spang Microanalytical Laboratory, Ann Arbor, Mich.) and from metal analyses by ignition to the oxide. *Anal.* Calcd for $La_2(CO_3)_3 \cdot 8H_2O$: La, 46.15; C, 5.98; H, 2.69. Found:

---

(1) M. L. Salutsky and L. L. Quill, *J. Am. Chem. Soc.*, **72**, 3306 (1950).

(2) R. G. Charles, *J. Inorg. Nucl. Chem.*, **27**, 1498 (1965).

(3) E. L. Head, 6th Rare Earth Research Conference, Gatlinburg, Tenn., May 1967.

(4) E. L. Head and C. E. Holley, Jr., "Rare Earth Research III," Gordon and Breach, New York, N. Y., 1964, p 51.

(5) E. L. Head and C. E. Holley, Jr., "Rare Earth Research IV," Gordon and Breach, New York, N. Y., 1965, p 707.

(6) R. L. N. Sastry, S. R. Yoganarisimhan, P. N. Mehrota, and C. N. R. Rao, *J. Inorg. Nucl. Chem.*, **28**, 1165 (1966).

(7) M. Clarus Strouth, Ph.D. Thesis, Michigan State University, 1962.

(8) G. Pannetier, J. Nataf, and A. Deireigne, *Bull. Soc. Chim. France*, **5**, 318 (1965).

(9) P. Caro and L. Eyring, personal communication.

(10) S. D. Ross and J. Goldsmith, *Spectrochim. Acta*, **20**, 781 (1964).

(11) D. Palache, H. Berman, and C. Frondel, "Dana's Systems of Mineralogy," Vol. II, 7th ed, John Wiley and Sons, Inc., New York, N. Y., 1944.